Title

Developing functional musculoskeletal tissues through hypoxia and lysyl oxidase-induced collagen cross-linking

Journal

Proceedings of the National Academy of Sciences of the United States of America, 111(45)

ISSN

0027-8424

Authors

Makris, Eleftherios A
Responte, Donald J
Paschos, Nikolaos K
et al.

Publication Date

2014-11-11

DOI

10.1073/pnas.1414271111

Peer reviewed

Developing functional musculoskeletal tissues through hypoxia and lysyl oxidase-induced collagen cross-linking

Eleftherios A. Makris[a], Donald J. Responte[a], Nikolaos K. Paschos[a], Jerry C. Hu[a], and Kyriacos A. Athanasiou[a,b,1]

Departments of [a]Biomedical Engineering and [b]Orthopedic Surgery, University of California, Davis, CA 95616

Edited* by Kyriacos C. Nicolaou, Rice University, Houston, TX, and approved September 30, 2014 (received for review July 29, 2014)

The inability to recapitulate native tissue biomechanics, especially tensile properties, hinders progress in regenerative medicine. To address this problem, strategies have focused on enhancing collagen production. However, manipulating collagen cross-links, ubiquitous throughout all tissues and conferring mechanical integrity, has been underinvestigated. A series of studies examined the effects of lysyl oxidase (LOX), the enzyme responsible for the formation of collagen cross-links. Hypoxia-induced endogenous LOX was applied in multiple musculoskeletal tissues (i.e., cartilage, meniscus, tendons, ligaments). Results of these studies showed that both native and engineered tissues are enhanced by invoking a mechanism of hypoxia-induced pyridinoline (PYR) cross-links via intermediaries like LOX. Hypoxia was shown to enhance PYR cross-linking 1.4- to 6.4-fold and, concomitantly, to increase the tensile properties of collagen-rich tissues 1.3- to 2.2-fold. Direct administration of exogenous LOX was applied in native cartilage and neocartilage generated using a scaffold-free, self-assembling process of primary chondrocytes. Exogenous LOX was found to enhance native tissue tensile properties 1.9-fold. LOX concentration- and time-dependent increases in PYR content (~16-fold compared with controls) and tensile properties (approximately fivefold compared with controls) of neocartilage were also detected, resulting in properties on par with native tissue. Finally, in vivo subcutaneous implantation of LOX-treated neocartilage in nude mice promoted further maturation of the neotissue, enhancing tensile and PYR content approximately threefold and 14-fold, respectively, compared with in vitro controls. Collectively, these results provide the first report, to our knowledge, of endogenous (hypoxia-induced) and exogenous LOX applications for promoting collagen cross-linking and improving the tensile properties of a spectrum of native and engineered tissues both in vitro and in vivo.

collagen cross-linking | tissue engineering | musculoskeletal tissues | lysyl oxidase | pyridinoline

Regenerative medicine and tissue engineering are providing new avenues to treat a multitude of conditions and diseases through restoring, maintaining, or enhancing the function of a wide range of tissues (e.g., muscle, bone, skin) and organs (e.g., heart, lungs, kidneys). Despite recent advancements, the clinical utility of many engineered tissues remains dependent upon the development of methods that promote mechanically robust tissues capable of withstanding the in vivo environment. This problem presents a critical hurdle for efforts geared toward developing de novo musculoskeletal tissues, such as cartilage, meniscus, tendons, and ligaments, for reparative and regenerative strategies. Tissue engineering has the potential to provide alternative treatment options for musculoskeletal injury and disease by generating neotissue that mimics the complex structure of native tissue (1, 2). The objective is to improve the properties of the engineered tissues to achieve native tissue biomechanical properties, maturation, and long-term functionality. For example, in articular cartilage tissue engineering, a variety of methods, including combinations of hydrostatic pressure and growth factor treatment (3), fluid flow (4), and matrix-modulating enzymes (5), have resulted in improved neotissues with tensile moduli ranging from 1.3 to 2.3 MPa; however, native tissue values range from 5 to 25 MPa (6). Similarly, in neofibrocartilage, tensile properties have been reported to be 2.5–3.5 MPa (7, 8), with native fibrocartilage values ranging from 7 to 295 MPa (9, 10). These low properties likely result from the immaturity of the ECM of the neotissues, which is mainly due to lack of collagen cross-links (11). Therefore, it is important that additional treatment modalities be evaluated toward enhancing neotissue tensile properties.

Collagen, the most prevalent fibrous protein in the body, supports the mechanical integrity of tissues and organs. In musculoskeletal tissues, collagen comprises the major fraction of the ECM and accounts for ~65–80% of these tissues' dry weights (12). After collagen biosynthesis and triple-helix formation, the copper-dependent enzyme lysyl oxidase (LOX) catalyzes extracellular modification of lysine and hydroxylysine amino acids of the collagen fibers into their aldehyde forms (Fig. 1*A*). Sequentially, this modification induces the formation of covalent pyridinoline (PYR) cross-links between individual collagen fibers (13) (Fig. 1*B*) and stabilizes the formation of heterotypic fibrils (Fig. 1*C*) and, subsequently, the tissue ECM. These intermolecular collagen cross-links, present in all native musculoskeletal tissues, signify the maturity of the tissue's ECM (14). In particular, cartilaginous tissues, ligaments, and tendons feature two forms of collagen cross-links, the difunctional (initial/immature) cross-link dehydrodihydroxylysinonorleucine and the trifunctional (mature) cross-link hydroxylysyl-PYR (15) (Fig. 1*B*). Several studies have highlighted the pivotal role of these cross-links in native tissues' biomechanical or functional properties (11, 16,

Significance

The inadequate mechanical properties of engineered tissues have prevented related therapies from clinical translation. Collagen cross-links correlate with the mechanical integrity of tissues; however, addressing the weakness of neotissues through enhancing collagen cross-links has not received the attention it deserves. The present study demonstrates, both in vitro and in vivo, that improvements in the mechanical properties of native and engineered tissues can be attained using endogenous (hypoxia-mediated) and exogenous application of lysyl oxidase, which is the enzyme responsible for collagen cross-linking. By promoting an ~16-fold increase in collagen cross-linking and, concomitantly, an approximately fivefold enhancement in the neotissue's mechanical properties, this work creates new prospects for regenerative medicine. The methods developed here work across a spectrum of collagen-rich tissues and are clinically applicable.

Author contributions: E.A.M., D.J.R., N.K.P., J.C.H., and K.A.A. designed research, performed research, contributed new reagents/analytic tools, analyzed data, and wrote the paper.

The authors declare no conflict of interest.

*This Direct Submission article had a prearranged editor.

[1]To whom correspondence should be addressed. Email: athanasiou@ucdavis.edu.

This article contains supporting information online at www.pnas.org/lookup/suppl/doi:10.1073/pnas.1414271111/-/DCSupplemental.

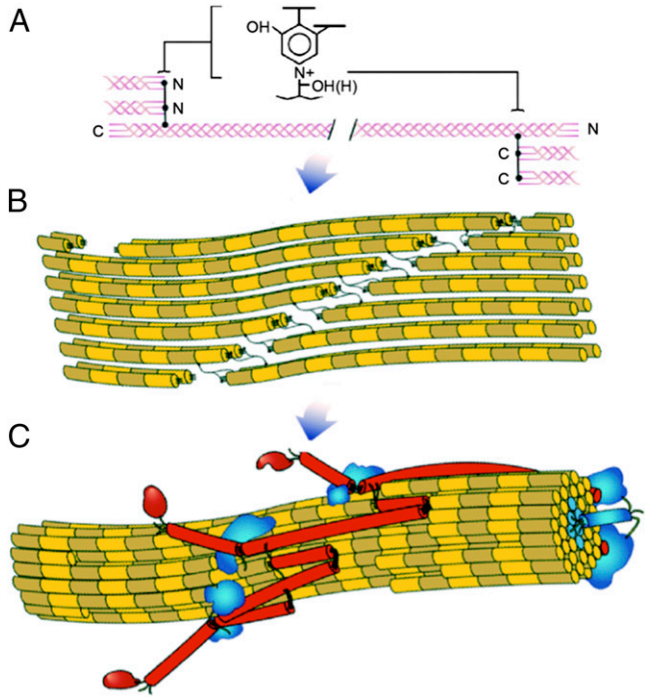

Fig. 1. This illustration represents a hierarchical depiction of a heterotypic collagen fibril that is commonly found in most musculoskeletal tissues, such as cartilage, tendons, and ligaments. The figure emphasizes the internal axial relationships required for the formation of mature cross-links. (*A*) Detailed view of the axial stagger of individual collagen molecules required for PYR cross-linking. (*B*) Illustration of relationships among neighboring axial fibers of trifunctional (mature) hydroxylysyl-PYR collagen cross-links. (*C*) Illustration of a 3D concept of a heterotypic fibril, commonly found in musculoskeletal tissues, consisting of collagen types II (yellow), IX (red), and XI (blue). Figure adapted from ref. 68.

17). For example, in cartilage, the cross-linked collagen fibrils noncovalently stabilize the highly hydrated, negatively charged proteoglycans (18). These findings suggest the need for recapitulating cross-linking in engineered collagen-rich tissues.

Only a few studies to date have evaluated the extent of collagen cross-links (19, 20) and, more importantly, their influence on the tensile and compressive properties of engineered musculoskeletal tissues. In contrast, many studies have investigated how other ECM components, such as glycosaminoglycan (GAG), collagen, and mineralization, contribute to biomechanical properties (19, 21–23). Such work has yielded variable results. Specifically, although it has been suggested that the compressive properties of native articular cartilage are best correlated with the proteoglycan component of the ECM (24), more recent studies have shown a better correlation of the compressive modulus with a combination of both GAG and collagen content (25–27). For engineered tissues, tensile stiffness has been strongly associated with total collagen content (22) as well as PYR content (28). Nevertheless, a significant correlation with compressive properties has also been reported with respect to the PYR content of engineered tissues (28). These findings might suggest that the various tissue biomechanical properties are dependent on more than just the quantity of specific biochemical components (29). Therefore, the unique structural organization, cross-linking, and architecture of the collagen network also likely play equally important roles, along with collagen and GAG quantities, in determining the biomechanical functionality of the tissue.

To the best of our knowledge, there are no validated and optimized methods for promoting collagen cross-linking and concomitant improvement in biomechanical properties in a spectrum of native and engineered tissues. Low oxygen tension, however, has been shown to have various molecular effects in different tissues (30, 31) through a hypoxia-dependent mechanism. This molecular mechanism is based on the critical involvement of hypoxia-inducible factor-1 (HIF-1) (32), which is present in many cells (33–35), including articular chondrocytes (36). In diarthrodial joints as well as developmental growth plates, chondrocytes experience hypoxic conditions (37). Low oxygen tension has been shown to affect the metabolism of articular chondrocytes, targeting the production of tissue-specific cartilage ECM proteins (38–42). Deletion of HIF-1α results in chondrocyte death, along with diminished expression of the cyclin-dependent kinase inhibitor p57, highlighting the importance of HIF-1 regulation for cell survival and growth arrest in this hypoxic environment (43). The critical role of HIF-1 in the chondrogenic differentiation of rat mesenchymal stem cells as well as human ES cells has been also identified (42, 44–46). Hypoxia-induced HIF-1 stabilization has been shown to control LOX regulation (47, 48), suggesting that hypoxia could affect ECM stabilization and tissue maturation through LOX-induced PYR cross-link formation. The manifold role of HIF-1 raises the intriguing idea that the ECM of native and engineered tissues and, concomitantly, their functional properties could be manipulated through hypoxia-mediated stimulation of HIF-1–regulated pathways, *LOX* gene expression, and sequential collagen cross-link formation.

Although studies have elucidated the pathway underlying the effects of hypoxia on cartilage growth, function, and synthesis, the ability of endogenous (hypoxia-induced) and exogenous LOX application to enhance collagen cross-linking and concomitant mechanical properties in both native and engineered tissues remains unexplored and is the central hypothesis of the present study. In the series of studies presented here, a variety of musculoskeletal tissues widely used in clinical practice as grafts to replace degenerative tissues as well as neocartilage constructs were investigated to assess hypoxia- and LOX-mediated collagen cross-linking manipulation. The overall goal was to preserve and promote the functional properties of the native explants and neotissues, respectively. Strategically targeting collagen cross-links may be useful for engineering tissues de novo, for elucidating disease processes, and for the development of potential novel therapeutic modalities.

Results

Hypoxia Enhances the Functional Properties of Articular Cartilage via LOX-Induced Collagen Cross-Linking. We first investigated the effects of continuous hypoxia (2% O_2) application on bovine articular cartilage explants during a 4-wk tissue culture period. The tensile (Young's) modulus of hypoxia-treated cartilage was 238% ($P = 0.007$) of control values (Fig. 2*A* and Table 1). No differences were observed in the tissue compressive (aggregate) modulus ($P > 0.05$) (Table 1). In addition, low oxygen tension increased the amount of PYR cross-links per wet weight (PYR/WW) and per collagen (PYR/Col) by 43% ($P = 0.04$) and 41% ($P = 0.03$), respectively, over controls (Fig. 2 *B* and *C*). A 44-fold increase in LOX gene expression ($P < 0.001$) was also detected (Fig. 2*D*). No differences were observed in Col/WW and GAG/WW ($P > 0.05$) (Table 1). By applying the LOX inhibitor β-aminopropionitrile (BAPN), the effects of hypoxia (increased tensile properties and PYR/WW) were abolished. Thus, continuous hypoxia application in articular cartilage promoted LOX gene expression, enhanced PYR collagen cross-linking, and subsequently improved the tensile properties of the cultured tissue.

Hypoxia Enhances the Functional Properties of Tendon, Ligament, and Meniscus via LOX-Induced Collagen Cross-Linking. A second study sought to determine whether hypoxia application could effectively preserve or improve the functional properties of other cultured musculoskeletal tissues via the same LOX-mediated

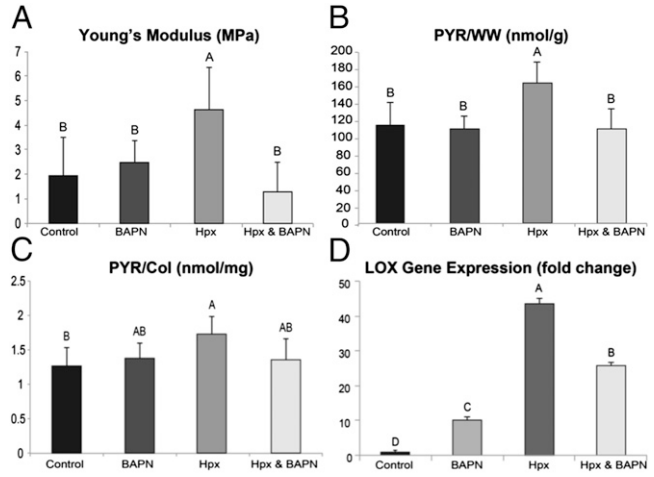

Fig. 2. Biomechanical and biochemical properties of articular cartilage treated with hypoxia (Hpx) and the LOX inhibitor BAPN for 4 wk. Tensile stiffness as represented by Young's modulus (*A*), PYR/WW (*B*), PYR/Col (*C*), and hypoxia-mediated LOX gene expression (*D*) are illustrated. Bars denote mean ± SD, and groups not connected by the same letter are significantly different ($P < 0.05$).

mechanism. Continuous hypoxia was applied to anterior cruciate ligament (ACL), posterior cruciate ligament (PCL), patellar tendon, and knee meniscus explants during a 4-wk tissue culture period. Similar to previous results, low oxygen tension application resulted in increases (140–643% and 152–340% of controls) in the tensile modulus and strength [ultimate tensile strength (UTS)] of a wide spectrum of musculoskeletal tissues (Fig. 3 *A* and *B* and Table 2), respectively. These increases were shown to occur through hypoxia-induced increases in PYR/WW and PYR/Col, which were enhanced 52–71% and 63–117%, respectively, over control values (Fig. 3 *C* and *D* and Table 2). Further addition of the LOX inhibitor BAPN resulted in partial or total abolishment of the measured differences generated from the application of hypoxia (tensile properties, PYR/WW, and PYR/Col). Interestingly, although hypoxia induced PYR cross-links in all examined tissues and had no effect on the collagen amount of ACL and patellar tendon ($P > 0.05$), it decreased the amount of collagen/WW in PCL ($P = 0.03$) and meniscus ($P = 0.04$) (Table 2). Thus, the effects of hypoxia application in various musculoskeletal tissues were manifested as increased tensile properties through PYR collagen cross-linking.

Exogenous LOX Application Affects the Functional Properties of Articular Cartilage via Collagen Cross-Linking. To identify alternative ways to induce PYR cross-linking, and thus enhance tissue functional properties, we investigated the effects of exogenous LOX application on the biochemical and biomechanical properties of cultured articular cartilage during a 2-wk tissue culture period. Findings of this study, which explored two different LOX concentrations, showed that 0.15 ng/mL LOX (high LOX) resulted in a tensile modulus and strength of articular cartilage at 186% ($P = 0.007$) and 185% ($P = 0.03$), respectively, of control values (Fig. 4 *A* and *B* and Table 1). No effects of LOX were detected on the aggregate modulus ($P > 0.05$). In addition, high LOX increased PYR/WW (204% of control values; $P = 0.03$) and PYR/Col (250% of control values; $P = 0.03$) (Fig. 4 *C* and *D* and Table 1). No effects were observed on collagen or GAG in the LOX-treated tissue over controls ($P > 0.05$) (Table 1). Thus, exogenous LOX application in cultured articular cartilage explants enhanced tissue tensile properties through PYR cross-linking.

Exogenous LOX Application Exerts Concentration- and Time-Dependent Effects on Neocartilage Formation. To refine further how collagen cross-links can be controlled during neocartilage development, the temporal modulation of exogenously applied LOX-induced collagen cross-linking was examined via two sequential phases using scaffold-free, self-assembled neocartilage as a representative model. In phase I, the effects of three different LOX concentrations were investigated. In phase II, the time dependence of LOX application was examined. For both phases, qualitative histological and immunohistochemical evaluation revealed that all neotissues produced uniform collagen and GAG, with a strong presence of collagen II (Fig. 5 *A* and *B*). In phase I, 0.15 μg/mL LOX increased the neotissue Young's modulus to 5.0-fold ($P < 0.001$) (Fig. 5*C* and Table 1) and PYR/WW to 16.2-fold ($P = 0.03$) (Fig. 5*D* and Table 1) of controls. No differences were observed in collagen and GAG content ($P > 0.05$). Phase II showed that early ($t = 8$–15 d) LOX application during neotissue formation increased by 288% the

Table 1. Biochemical content and biomechanical properties of native and engineered articular cartilage

Study	Group	E_Y, MPa	UTS, MPa	H_A, MPa	Col/WW, %	GAG/WW, %	PYR/WW, nmol/g
Hypoxia in articular cartilage	Control	2.0 ± 1.5^B	1.3 ± 1.1^B	0.51 ± 0.37	9.1 ± 1.5	5.2 ± 0.8	113.3 ± 26.4^B
	BAPN	2.5 ± 1.0^B	2.3 ± 0.7^B	0.38 ± 0.24	8.2 ± 2.4	5.0 ± 1.2	108.7 ± 17.5^B
	Hypoxia	4.6 ± 1.7^A	3.0 ± 1.0^A	0.43 ± 0.24	9.5 ± 2.1	5.9 ± 1.2	163.0 ± 13.8^A
	Hypoxia and BAPN	1.3 ± 1.2^B	2.0 ± 0.5^B	0.49 ± 0.25	8.1 ± 1.6	5.4 ± 0.5	109.2 ± 21.0^B
Exogenous LOX in articular cartilage	$t = 0$	12.7 ± 1.2^A	8.4 ± 1.2^A	0.67 ± 0.25	13.6 ± 1.4^A	8.0 ± 1.0	N/I*
	Control	6.6 ± 2.4^B	2.9 ± 1.7^C	0.52 ± 0.23	5.6 ± 2.5^B	8.4 ± 0.6	176.5 ± 67.6^B
	Low LOX	7.7 ± 2.7^B	3.2 ± 1.7^C	0.49 ± 0.26	7.5 ± 2.7^B	8.4 ± 0.8	206.1 ± 88.4^B
	High LOX	12.3 ± 3.4^A	5.4 ± 1.5^B	0.58 ± 0.17	5.8 ± 2.8^B	8.4 ± 0.7	395.3 ± 122.9^A
Exogenous LOX in neocartilage (phase I)	Control	0.4 ± 0.1^C	0.2 ± 0.0^C	0.13 ± 0.03	1.8 ± 0.2	1.1 ± 0.1	3.1 ± 1.5^C
	Low LOX	1.0 ± 0.3^B	0.3 ± 0.0^B	0.11 ± 0.020	1.6 ± 0.2	1.5 ± 0.4	20.6 ± 3.7^B
	Medium LOX	1.1 ± 0.2^B	0.3 ± 0.0^B	0.11 ± 0.01	1.8 ± 0.2	1.2 ± 0.1	26.6 ± 5.7^B
	High LOX	2.2 ± 0.7^A	0.5 ± 0.1^A	0.12 ± 0.02	1.9 ± 0.3	1.4 ± 0.4	35.4 ± 8.9^A
Exogenous LOX in neocartilage (phase II)	Control	0.4 ± 0.1^C	0.2 ± 0.0^B	0.10 ± 0.05^B	1.7 ± 0.2	1.8 ± 0.2	2.2 ± 0.6^B
	Early LOX	2.3 ± 0.8^A	0.5 ± 0.1^A	0.22 ± 0.05^A	1.8 ± 0.2	1.6 ± 0.1	26.1 ± 14.2^A
	Late LOX	0.8 ± 0.1^B	0.4 ± 0.2^A	$0.18 \pm 0.06^{A,B}$	1.8 ± 0.1	1.7 ± 0.1	35.1 ± 8.0^A

Values are mean ± SD. Groups not connected by the same letter (A, B, or C) are significantly different ($P < 0.05$). E_Y, Young's modulus; H_A, aggregate modulus. *Data are not included (N/I) here because they were collected and published in a previous study (69).

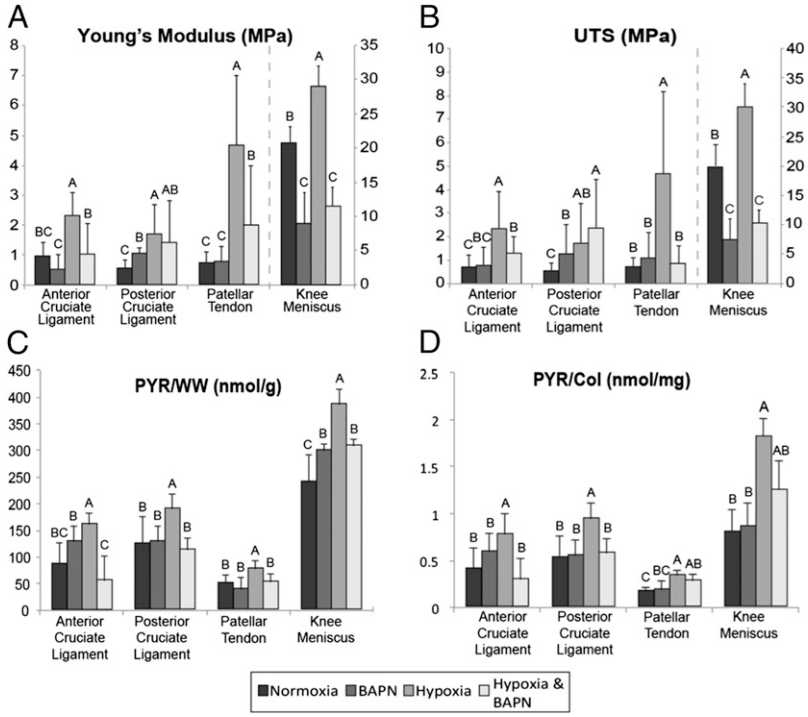

Fig. 3. Biomechanical and biochemical properties of ACL, PCL, patellar tendon, and knee meniscus treated with Hpx and the LOX inhibitor BAPN for 4 wk. Tensile stiffness as represented by Young's modulus (*A*), UTS (*B*), PYR/WW (*C*), and PYR/Col (*D*) is illustrated. Bars denote mean ± SD, and groups not connected by the same letter are significantly different ($P < 0.05$).

tensile modulus ($P < 0.001$) over late ($t = 15$–21 d) LOX application. The tensile modulus of early LOX-treated neotissue was 5.3-fold that of controls ($P < 0.001$) (Fig. 5*E* and Table 1). Additionally, both treatments increased the aggregate modulus of the neotissue by 100% of controls ($P = 0.02$) (Fig. 5*F* and Table 1). The LOX-treated groups also exhibited concomitant increases in the amount of PYR cross-links (16.0-fold of controls; $P = 0.003$) (Fig. 5*G* and Table 1). No effects were detected in the collagen and GAG content of the tissue ($P > 0.05$). In this study, the most potent effects on neotissue functional properties were due to the early application ($t = 8$–15 d) of the high concentration (0.15 μg/mL) of LOX.

To put the neocartilage's functional properties in perspective with native tissue values, we examined the biomechanical properties of cartilage explants immediately after harvesting. Under compression, the aggregate modulus of native, juvenile cartilage

Table 2. Biochemical content and biomechanical properties of native and engineered musculoskeletal tissues

Study	Group	E_Y, MPa	UTS, MPa	Col/WW, %	PYR/WW, nmol/g
Hypoxia in ACL	$t = 0$	7.3 ± 3.8	5.0 ± 3.6	14.4 ± 3.2	N/I*
	Control	0.9 ± 0.4^{BC}	0.7 ± 0.4^{C}	13.6 ± 2.9	95.3 ± 42.4^{BC}
	BAPN	0.5 ± 0.4^{C}	0.7 ± 1.0^{BC}	14.0 ± 4.3	128.7 ± 28.7^{B}
	Hypoxia	2.3 ± 0.7^{A}	2.3 ± 0.7^{A}	13.6 ± 2.0	161.2 ± 22.0^{A}
	Hypoxia and BAPN	1.0 ± 0.8^{B}	1.3 ± 0.6^{B}	12.6 ± 0.9	56.0 ± 45.5^{C}
Hypoxia in PCL	$t = 0$	12.8 ± 6.0	12.8 ± 6.0	16.2 ± 1.7	N/I*
	Control	0.5 ± 0.3^{C}	0.5 ± 0.3^{C}	15.1 ± 2.1^{A}	124.9 ± 50.3^{B}
	BAPN	1.0 ± 0.1^{B}	1.2 ± 0.4^{B}	16.1 ± 2.4^{A}	128.4 ± 29.4^{B}
	Hypoxia	1.7 ± 0.9^{A}	1.7 ± 0.9^{AB}	13.7 ± 1.3^{B}	190.2 ± 27.3^{A}
	Hypoxia and BAPN	1.4 ± 0.6^{AB}	4.2 ± 2.5^{A}	12.2 ± 1.9^{B}	113.4 ± 22.7^{B}
Hypoxia in patellar tendon	$t = 0$	23.7 ± 13.3	13.3 ± 6.5	15.2 ± 2.1	N/I*
	Control	0.7 ± 0.3^{C}	0.7 ± 0.3^{B}	14.2 ± 3.1^{A}	45.4 ± 13.0^{A}
	BAPN	0.7 ± 0.5^{C}	1.0 ± 0.7^{B}	11.2 ± 1.7^{B}	39.5 ± 22.8^{B}
	Hypoxia	4.6 ± 2.3^{A}	2.3 ± 2.0^{A}	15.6 ± 1.2^{A}	77.8 ± 14.7^{A}
	Hypoxia and BAPN	2.0 ± 1.6^{B}	0.8 ± 0.7^{B}	10.4 ± 1.8^{B}	52.9 ± 16.9^{B}
Hypoxia in knee meniscus	$t = 0$	49.5 ± 10.0	14.6 ± 6.7	24.1 ± 2.2	N/I*
	Control	20.7 ± 2.4^{B}	19.8 ± 3.6^{B}	23.2 ± 2.8^{A}	239.6 ± 51.3^{A}
	BAPN	9.0 ± 4.5^{C}	7.4 ± 3.6^{C}	23.0 ± 1.7^{A}	278.6 ± 52.5^{A}
	Hypoxia	29.0 ± 3.0^{A}	30.0 ± 4.0^{A}	17.9 ± 2.2^{B}	386.1 ± 28.8^{B}
	Hypoxia and BAPN	11.5 ± 2.7^{C}	10.3 ± 2.3^{C}	19.8 ± 3.9^{B}	308.4 ± 13.5^{B}

Values are mean ± SD. Groups not connected by the same letter (A, B, or C) are significantly different ($P < 0.05$).
*N/I data are not included here because they were collected and published in a previous study (69).

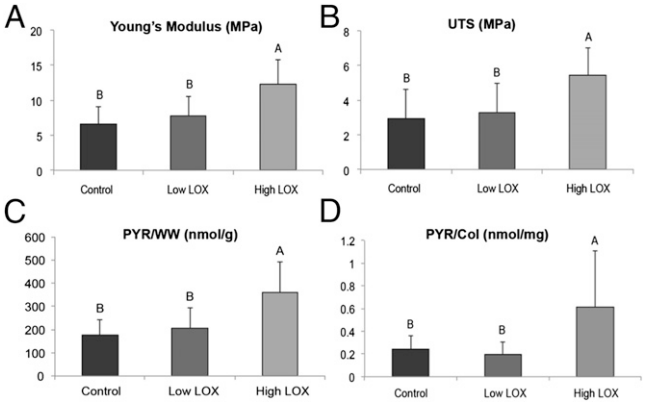

Fig. 4. Biomechanical and biochemical properties of articular cartilage treated with LOX at concentrations of 0.0015 ng/mL (low LOX) and 0.15 ng/mL (high LOX). Tensile stiffness as represented by Young's modulus (*A*), UTS (*B*), PYR/WW (*C*), and PYR/Col (*D*) is illustrated. Bars denote mean ± SD, and groups not connected by the same letter are significantly different ($P < 0.05$).

was 0.28 ± 0.07 MPa. The aggregate modulus of 6-wk-old neocartilage treated with LOX, tested under the same conditions (thickness and strain), was 0.22 ± 0.05 MPa. Thus, the values of LOX-treated constructs were ∼80% of the native tissue's values. Similarly, under tension, the tensile modulus of the native cartilage was 5.0 ± 1.9 MPa. The tensile modulus of the LOX-treated neotissue was 2.3 ± 0.8 MPa. Thus, neocartilage's Young's modulus represented ∼50% of the native tissue's values.

Effects of Exogenous LOX on ECM Maturation and Neocartilage Functional Properties Continue in Vivo. Motivated by the in vitro results of the previous study, we sought to translate these effects in vivo. Control and LOX-treated neotissues were grown in vitro for 6 wk and then implanted s.c. into the backs of athymic mice for an additional 6 wk. Histological evaluation of explanted neotissues (Fig. S1) using Masson's trichrome revealed uniform collagen staining in all constructs. In addition, there was no overt histological evidence of a fibrous capsule around the cartilage constructs. Immunohistochemistry (IHC) found positive collagen II and negative collagen I staining. Immunostaining for CD68 macrophage transmembrane glycoprotein and histomorphological evaluation showed no overt evidence of inflammatory cell (macrophage) infiltration within neocartilage. Similarly, immunostaining for CD31 endothelial surface protein indicated no overt evidence of neovascularization within the engineered cartilage. Quantitative evaluation of SEM images revealed the in vivo environment to increase fibril density of control neotissues by 23% over those neotissues maintained in vitro ($P = 0.002$) (Fig. 6*A* and Table S1). In addition, although all LOX-treated neotissues presented with enhanced fibril density, the implanted LOX-treated neocartilage had a fibril density of 34% over in vitro neocartilage controls ($P < 0.001$) (Fig. 6*B* and Table S1). In terms of fibril diameter, no significant differences were observed among the groups ($P > 0.05$) (Fig. 6*C* and Table 1).

The in vivo growth environment increased the amount of Col/WW in both control and LOX-treated groups by 18% and 16%, respectively, over in vitro controls ($P = 0.04$) (Fig. 7*A* and Table S1). No significant differences were observed in the amount of GAG/WW among all groups ($P > 0.05$). The in vivo LOX-treated group exhibited PYR/WW 14-fold the in vitro control values ($P < 0.001$) (Fig. 7*B* and Table S1). The in vivo implants had increased tensile modulus and strength of 72% and 26%, respectively, over their in vitro counterparts (Fig. 7*C* and Table S1). The in vivo LOX-treated constructs displayed an increased tensile modulus that was threefold greater than the tensile modulus of in vitro control values ($P < 0.001$). In terms of compressive modulus, the in vivo environment again provided a significant benefit over in vitro culture ($P = 0.04$) (Fig. 7*D* and Table S1).

Discussion

These experiments describe different methods for promoting collagen cross-linking in both native and engineered tissues. Specifically, hypoxia was shown to preserve and/or induce collagen cross-links and biomechanical properties in a spectrum of musculoskeletal tissues when maintained on a long-term basis in tissue culture. These tissues, frequently used in clinical practice as grafts for replacing degenerative tissues, deteriorate during storage. It was found that up-regulation of hypoxia-induced LOX increased PYR cross-links and, concomitantly, increased tensile properties of articular cartilage, knee meniscus, patellar tendon, ACL, and PCL. As a next step, the effects of exogenous LOX application were investigated in both native articular cartilage and neocartilage. In doing so, an optimal concentration (0.15 μg/mL) and application time (t = 8–15 d) of LOX were identified that enhance collagen cross-linking and tissue functional properties. LOX was shown to be directly responsible for the formation of PYR cross-links in cartilage and neotissue, without any deleterious effects on the ECM. These results were found to be translatable to the in vivo environment, where s.c. implantation of LOX-treated neotissue resulted in higher PYR cross-links and, concomitantly, greater functional properties. Thus, LOX application presents as a promising tool to modulate collagen cross-linking and the functional properties of native and engineered tissues.

The systematic examination of the effects of low oxygen tension on growth and remodeling of in vitro-cultured tissues provides a mechanistic description of hypoxia-induced PYR cross-linking formation and tissue biomechanical property enhancement. Based on previous findings and the results of the present study, it is hypothesized that hypoxia stabilizes HIF-1α (49) and promotes HIF-1–mediated LOX up-regulation (47, 48), which, in turn, catalyzes the formation of PYR cross-links (50) to result in enhanced tissue functional properties. This mechanism adds to the already known roles of HIF-1 on chondrocyte metabolism (37), ECM protein synthesis (38–42), and chondrogenic differentiation of mesenchymal and human ES cells (42, 44–46). Considering the beneficial effects of hypoxia toward the functional properties of the various musculoskeletal tissues investigated here, this hypothesis appears to be translatable across other collagen-rich tissues.

In addition to inducing endogenous cross-link formation, the present findings indicate that hypoxia exerts potentially undesirable effects upon the matrix components of musculoskeletal tissues. Previous work has connected hypoxia application with the up-regulation of the cartilage-specific transcriptional factor SRY (sex determining region Y)-box 9 (SOX-9), which directly regulates several important matrix genes, such as those matrix genes encoding Col-2a1, aggrecan, and Col-9 (41, 42). However, in the present study, continuous hypoxia application (2% O_2) was shown to decrease the amount of collagen in the PCL and knee meniscus. These findings can be partially explained by the fact that both of these tissues have vascularized regions. Specifically, the knee meniscus is well vascularized in the outer portion (51), and the PCL ligament has rich vascularization in the distal part (52). The presence of a blood supply may cause the cells in these regions to have a highly O_2-dependent metabolism. It is hypothesized that the hypoxic environment may not have satisfied the physiological O_2 requirements of the meniscus and PCL cells, which may explain the deleterious effects of hypoxia on the collagen content of these tissues. Future studies need to elucidate the effects of different levels of O_2 on the biochemical and functional properties of these tissues.

Exogenous LOX application provides a successful method to preserve or improve the properties of cartilage explants maintained in tissue culture. Collagenous grafts and explants intended

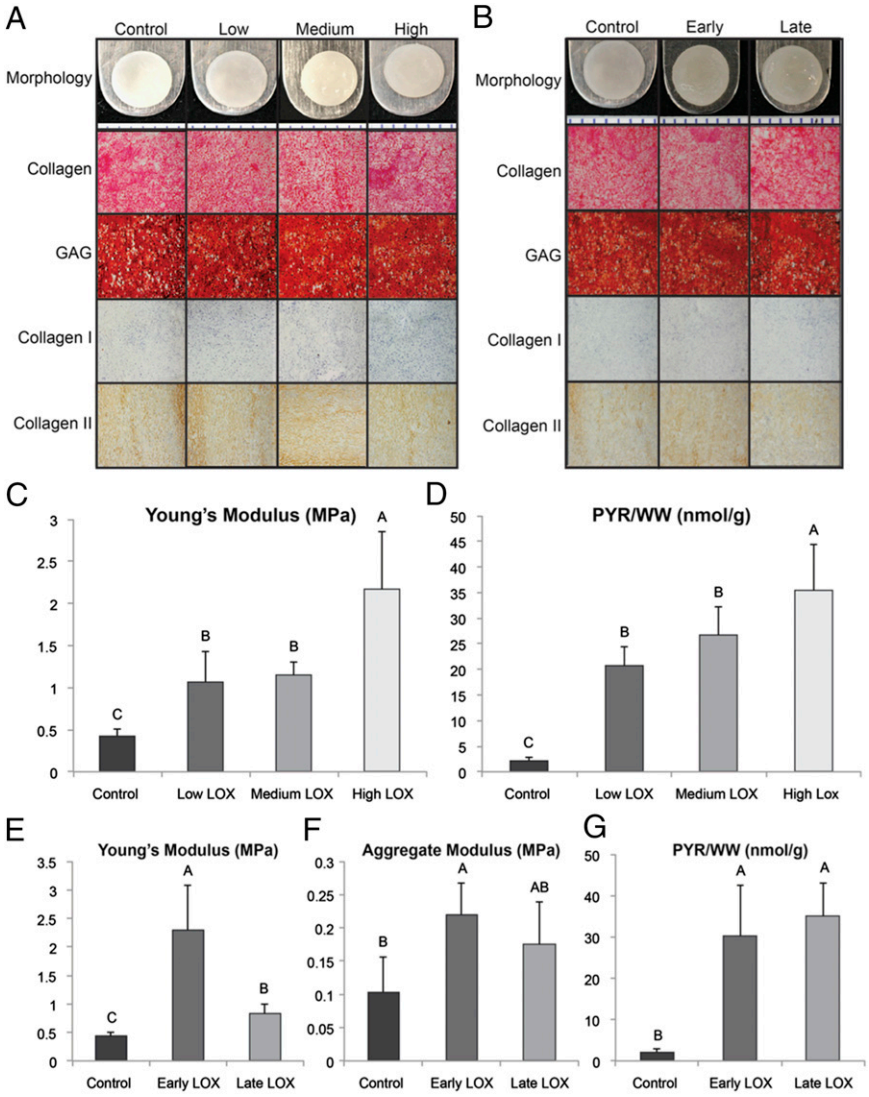

Fig. 5. Gross morphology, histology, IHC, biomechanical properties, and biochemical content of neocartilage treated with LOX. (*A*, *C*, and *D*) In phase I, LOX was applied at three concentrations: low (0.0015 μg/mL), medium (0.015 μg/mL), and high (0.15 μg/mL). (*B* and *E*–*G*) In phase II, the high LOX treatment was applied for $t = 8$–14 d (early LOX) or $t = 15$–21 d (late LOX) during a 6-wk culture period to examine temporal effects. Histology staining for collagen and GAG, and IHC staining for collagen types II and I (*A* and *B*), Young's modulus for phase I (*C*), PYR content normalized to neotissue WW (PYR/WW) for phase I (*D*), Young's modulus for phase II (*E*), an aggregate modulus for phase II (*F*), and PYR/WW for phase II (*G*) are illustrated. Bars denote mean ± SD, and groups not connected by the same letter are significantly different ($P < 0.05$).

for implantation or reconstruction are often stored in culture media. However, it is known that the material properties of these grafts deteriorate with time. Serum-supplemented medium causes tissue swelling (53) and dedifferentiation (54), as well as cellular outgrowth (55). Although a chemically defined, serum-free medium has been introduced specifically to avoid these deleterious effects, properties of stored tissues still remain inferior compared with native tissue values (56, 57). In the present study, a chemically defined serum-free medium supplemented with LOX was found to result in the maintenance, if not improvement, of graft properties. In addition to the role of collagen cross-links in a tissue's biomechanical properties, some studies have highlighted how PYR reduces collagen type II catabolism (11, 58). The presence of PYR in the ECM reduces susceptibility to matrix degradation due to matrix metalloproteinase-1 (MMP-1) (11). In parallel, it has been reported that matrices produced by skin fibroblasts with more PYR cross-links were less susceptible to MMP-1 degradation (58). Therefore, promoting PYR cross-linking in native tissues through exogenous LOX application might provide a way to prevent explant degeneration. Thus, in terms of clinical applicability, it may be advisable to consider LOX supplementation during storage or transport of collagenous grafts intended for implantation.

Although osteochondral implants are beneficial in treating cartilage-degenerative pathologies and are widely used in clinical practice, they are limited in supply and can lead to donor site morbidity, and their success is greatly hindered by their inability to integrate with host tissue upon implantation (59). Thus, efforts to develop metabolically active engineered replacements capable of adapting to and integrating with the in vivo environment have gained tremendous interest. The major hurdle in developing such neotissues in vitro is achieving a structurally robust ECM with sufficient mechanical properties. Indeed, the US Food and Drug Administration guidance document for knee cartilage repair lists the "ability of the implant to withstand expected in vivo…loading" as a key success criterion for the

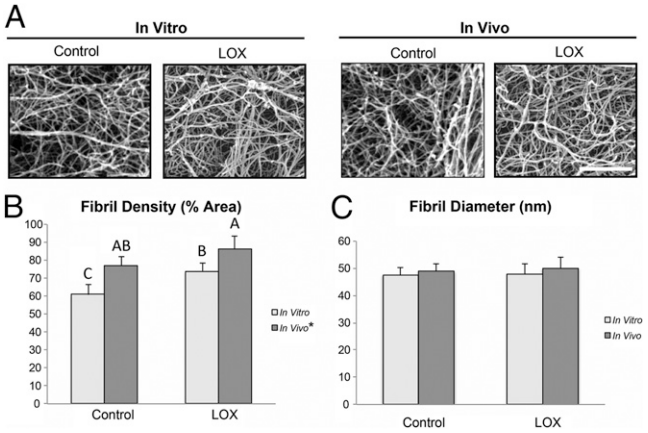

Fig. 6. (*A*) SEM of neocartilage after 6 wk of implantation in nude mice compared with in vitro controls. (Scale bar, 1 μm.) (*B*) Evaluation of fibril diameter of the neotissue. (*C*) Evaluation of fibril diameter of neocartilage. Bars denote mean ± SD, and groups not connected by the same letter are significantly different (*$P < 0.05$).

preclinical evaluation of repair products (60). Exogenous LOX application provides an alternative method for the modulation of collagen cross-linking in neotissues. Refining the window of LOX application to an earlier time point (8–15 d vs. 15–21 d) allowed us to tailor the beneficial effects, increasing both the tensile and compressive properties of the neotissue. Because LOX acts using a completely different mechanism than other currently used stimuli, such as hydrostatic pressure, direct compression, or growth factors, it could be combined with these stimuli to produce synergistic effects, and thus further promote tissue functional properties. Collectively, these results illustrate an important step toward producing neotissue that is suitable for preclinical work.

Although the exact molecular pathways of endogenous LOX gene expression and mediation in collagen cross-linking formation in different tissues are not fully elucidated, these processes seem to take place at the initial stages of collagen growth and maturation (61). By investigating the effects of exogenously applied LOX on self-assembled neotissue, whose in vitro development recapitulates features of native cartilage morphogenesis (1, 2), this study provides insight into the role of endogenous LOX expression and regulation in native cartilage development. For both self-assembled neocartilage and native cartilage during morphogenesis, the initially ubiquitous collagen type VI localizes around the pericellular matrix, whereas collagen type II production rises. Although qualitative data showed LOX localization in cartilage during development, quantitative data for LOX expression do not exist, making it difficult to evaluate its developmental role. The present study showed that LOX-induced tensile increases are time-dependent, suggesting that endogenous LOX regulation during morphogenesis is timed to correspond with temporal changes in collagen types, eventually resulting in optimized tensile properties. Future studies should focus on shedding light onto these important aspects of collagen growth and maturation during in vivo morphogenesis and in vitro development of engineered tissues.

Pivotal to the development of strategies that result in functional replacement tissues is to investigate the effects of the in vivo environment on neotissue growth and development. The in vivo growth environment could prove beneficial for engineered tissue maturation because it provides the neotissue with nutrients, growth factors, and stimuli not applied in tissue culture, thus enhancing its biochemical and functional properties (23). Therefore, an additional study was performed to investigate the maturation potential of the in vivo environment in neotissue growth and development. Moreover, this study was conducted to explore the potential of a LOX pretreatment in an in vivo model to promote further neotissue maturation. Results indeed found an in vitro LOX pretreatment to carry over a significant effect into an in vivo model, resulting in enhanced maturation in terms of the tensile modulus and PYR content over in vitro-grown tissue. No discernable capsule and no appreciable cellular infiltration were found around the implanted neotissue, suggesting a minimal host response to the LOX-treated neotissue. Such work speaks to the potential of LOX as a potent agent for promoting not only in vitro but also in vivo neotissue maturation, suggesting a pivotal role of PYR cross-links in the pre- and postimplanted tissue.

In conclusion, the present series of studies demonstrate that hypoxia and exogenous LOX application promote collagen cross-linking and maturation, resulting in concomitant increases in the functional properties of collagen-rich tissues (Fig. 8). This work has produced several previously unidentified findings demonstrating (*i*) biochemical and biomechanical effects of hypoxia on a spectrum of collagen-rich tissues, (*ii*) potential mechanisms underlying the effects of hypoxia, (*iii*) biochemical and biomechanical effects of exogenous LOX application on native and engineered cartilage, (*iv*) the identification of an optimal concentration and application time of LOX for tissue engineering purposes, and (*v*) the influence of a LOX pretreatment on the in vivo development and maturation of neotissue. It is anticipated that hypoxia or exogenous LOX can be used to improve or maintain the mechanical properties of transplantation grafts, such as osteochondral tissue, meniscal tissue, sinews, and possibly any other highly collagenous tissue. With several growth factors and mechanical stimuli being identified to increase the biochemical content and compressive properties of engineered tissues, and with few methods existing to improve tensile properties, this study contributes to tissue engineering approaches by introducing collagen cross-linking methods that augment tensile properties. Moreover, LOX pretreatment promotes in vivo development and maturation of neotissue, resulting in further increases in its tensile properties postimplantation. The ability of LOX to be applied exogenously and to promote tissue maturation may allow for direct in vivo applications to treat defects or pathologies, such as via intraarticular injections. Overall, the results of this study demonstrate that endogenous (hypoxia-mediated) and exogenous LOX application provide exciting new technologies for promoting collagen network maturation and enhancement of the functional properties in both native and engineered tissues.

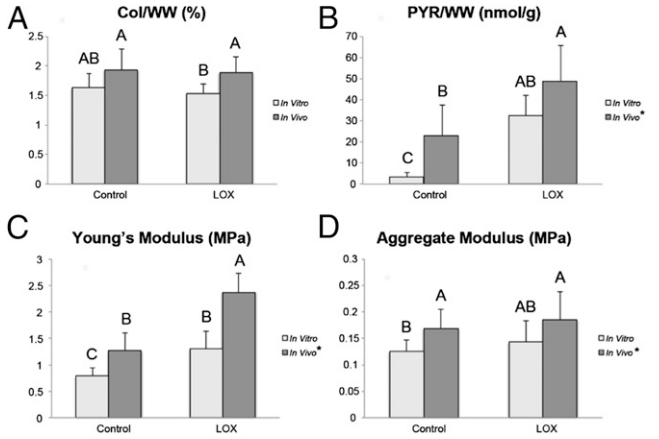

Fig. 7. Properties of neocartilage after 6 wk of implantation in nude mice compared with in vitro controls. Col/WW (*A*), PYR/WW (*B*), Young's modulus (*C*), and an aggregate modulus (*D*) are illustrated. Bars denote mean ± SD, and groups not connected by the same letter are significantly different (*$P < 0.05$).

Materials and Methods

Sample Preparation. Explants (trochlea groove cartilage, middle part of ACL, middle part of PCL, middle part of patellar tendon, and middle zone of medial meniscus) were harvested from the knee joint of eight calves ranging from 4–8 wk of age (four male calves and four female calves; Research 87). Explants were either analyzed immediately or incubated for 24 h before analysis.

Explant Culture. To investigate the effect of hypoxia on musculoskeletal tissues, two different types of media were used for explant culture: (*i*) cell culture medium [DMEM with low glucose (1 g/L); Life Technologies], 10% FBS (Atlanta Biologicals), 1% nonessential amino acids (Life Technologies), 25 mg of L-ascorbic acid (Sigma–Aldrich), and 1% penicillin/streptomycin/Fungizone (BioWhittaker) or (*ii*) cell culture medium supplemented with 0.25 mM BAPN (Sigma–Aldrich). Explants were divided into four treatment groups and cultured for 4 wk: control, BAPN, hypoxia, or hypoxia and BAPN. Explants in the control and BAPN groups were incubated in 10% CO_2 and 21% (vol/vol) O_2 at 37 °C. Explants receiving hypoxia were incubated separately in 2% (vol/vol) O_2 using a hypoxic incubator (Thermo Fisher Scientific) that develops hypoxic conditions through appropriate nitrogen regulation, keeping CO_2 constant at 10% (vol/vol).

Cell Isolation. Articular cartilage, harvested from the distal femur of six calves ranging from 4–8 wk of age (three male calves and three female calves) was digested in 0.2% collagenase type II (Worthington) for 18 h. Cells were isolated, frozen at −80 °C for 24 h in medium supplemented with 10% DMSO at 30 million cells per milliliter, and stored in liquid nitrogen until needed for seeding.

Neocartilage Culture. Neocartilage was formed using a self-assembling process as previously described (62). Briefly, primary chondrocytes were thawed; counted with a trypan blue exclusion test for viability; seeded into cylindrical nonadherent agarose wells; and fed with chondrogenic medium DMEM, 1% nonessential amino acids, 100 nm dexamethasone (Sigma–Aldrich), 1% ITS + (insulin, transferrin, selenium) premix (BD Scientific), 40 mg/mL L-proline (Sigma–Aldrich), 50 mg/mL ascorbate-2-phosphate (Sigma–Aldrich), 100 mg/mL sodium pyruvate (Fischer Scientific), 0.146 mg/mL hydroxylysine (Sigma–Aldrich), 0.0016 mg/mL copper sulfate (Sigma–Aldrich), and 1% penicillin/streptomycin/Fungizone initially for 4 h after self-assembly and then every 24 h.

In Vivo Study. The animal study was conducted under approval from the Institutional Animal Care and Use Committee, University of California, Davis.

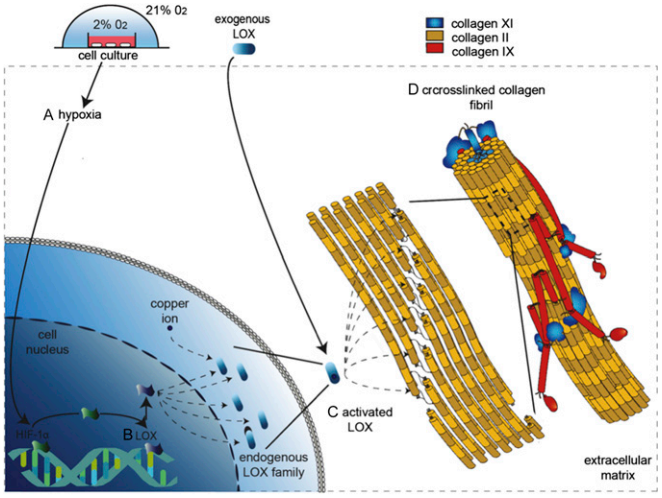

Fig. 8. Mechanistic description of HIF-1–mediated PYR collagen cross-linking formation toward enhancing biomechanical properties in native and engineered collagen-rich tissues. (A) Hypoxia application during tissue culture promotes HIF-1–mediated endogenous LOX gene expression. (B) Upregulation of LOX gene expression results in different LOX enzymes (LOX-1, LOX-2, LOX-3, LOX-4, and LOX-propeptide). (C) Collagen maturation occurs through extracellular modification of the collagen fibers by LOX, resulting in the formation of covalent PYR cross-links. Exogenous LOX application can promote the same effects, bypassing the side effects of hypoxia. (D) LOX (endogenous and exogenous)-mediated PYR cross-linking formation enhances functional properties of native and engineered tissues.

Both LOX-treated and control constructs were grown for 6 wk in vitro before being implanted s.c. into seven 6- to 8-wk-old athymic male mice. To implant the neotissue, general anesthesia was administered by mask to the mice using isoflurane, and a 3-mm incision was made down the centerline of the back of each mouse. From this incision, two s.c. pouches were created on either side of the thorax. Each mouse received a LOX-treated neotissue in one pouch and a control neotissue in the other, randomized with respect to left and right; staples were used to close the incision. The mice were humanely killed 6 wk later, at which point the neotissue was carefully removed from the s.c. pouches for analysis. In parallel with the in vivo study, control and LOX-treated tissues were also simultaneously grown in vitro for comparison.

LOX Application in Native and Engineered Cartilage. Articular cartilage explants were fed with chondrogenic medium supplemented with LOX (GenWayBio) at two concentrations, low (0.0015 μg/mL) and high (0.15 μg/mL), during a 2-wk culture period. In neocartilage, phase I investigated the effects of three different LOX concentrations, low (0.0015 μg/mL), medium (0.015 μg/mL), and high (0.15 μg/mL), during a 4-wk culture period. LOX-treated groups received LOX medium during t = 8–21 d after cell seeding. In phase II, two LOX treatment windows were evaluated using the concentration identified in phase I (i.e., 0.15 μg/mL): control, early LOX (applied t = 8–14 d), and late LOX (applied t = 15–21 d) during a 6-wk culture period.

Gross Morphology. ImageJ (NIH) software was used to determine the diameter and thickness of each sample. The central 3 mm of each construct was removed using a dermal biopsy punch for creep indentation testing, whereas the outer ring was divided for tensile testing, histology, and quantitative biochemistry, as previously described (62).

Histology and IHC. For histology, constructs were cryoembedded at −0 °C in HistoPrep (Fischer Scientific), sectioned at 14 μm, and fixed in 10% formalin. Neocartilage samples of the in vitro study were stained using Safranin-O/fast green for GAG or Picrosirius red for collagen. In the in vivo study, all samples were stained with Masson's trichrome to evaluate collagen structure, fibrous encapsulation, and inflammation. For IHC, sections were fixed in acetone at 4 °C. All constructs were immunostained for collagen types I and II to evaluate phenotypic maintenance. The in vivo study constructs were additionally immunostained for CD31, an endothelial surface protein, to investigate potential endothelial cell infiltration or neovascularization within or around the neotissue. IHC was also performed for CD68, a macrophage transmembrane glycoprotein, to investigate potential cellular infiltration within or around the neotissue. In vitro samples served as negative controls. Briefly, following antigen retrieval, samples were incubated with 3% H_2O_2 to quench endogenous peroxidase. Samples were then blocked with horse serum (Vectastain ABC kit; Vector Labs) and incubated with mouse anti-collagen type I (Accurate Chemicals), rabbit anti-collagen type II (Cedarlane Labs), mouse anti-CD31 (clone JC70A, M0823; Dako), or mouse anti-CD68 (clone 514H12, NCL-CD68; Novacastra) antibodies. Corresponding secondary antibodies, Vectastain ABC (Vector Laboratories) and 3,3′-diaminobenzidine (Vector Laboratories) solutions, were then used following the manufacturers' instructions. Staining was performed at the Veterinary Teaching Hospital of the University of California, Davis, and blinded evaluation was performed by two board-certified veterinary pathologists.

Quantitative Biochemistry. Samples were weighed, frozen, and lyophilized, and dry weights were also recorded. Samples were then digested in phosphate buffer with 5 mm of EDTA, 5 mm of *N*-acetyl-cysteine, and 125 μg/mL papain (Sigma–Aldrich) for 18 h at 65 °C. Following digestion of the samples, total collagen was quantified using a chloramine-T hydroxyproline assay; sulfated GAG of articular cartilage and neocartilage was quantified using the Blyscan Glycosaminoglycan Assay (Biocolor); and the total number of cells was estimated with a Picogreen DNA Assay (Molecular Probes) assuming 7.7 pg of DNA per cell, as previously described (63).

Real-Time PCR. To study hypoxia-induced gene expression, real-time RT-PCR was used. Past work has found LOX gene expression to change as early as 18 h following exposure to hypoxic conditions (47, 48). Following a 24-h incubation in normoxic conditions, articular cartilage explants were subjected to hypoxia for 24 h. Immediately after this exposure to hypoxia, LOX gene expression was measured. Briefly, total RNA was extracted using the Ambion RNAqueous kit (Life Technologies). RNA concentration and purity were measured on a Nanodrop spectrophotometer (Nanodrop Technologies). Then, following the manufacturer's instructions, 500 ng of RNA was incubated with SuperScript III reverse transcriptase (Life Technologies) in 25 μL of RNase-free water. SYBR Green Master Mix (Qiagen) and 1 μm of primers were used

on a Rotor-Gene 3000 real-time RT-PCR machine (Corbett Research) to perform a 10-min denaturing step, after which 45 cycles at 95 °C (for 15 s) and 60 °C (for 60 s) were conducted. To analyze the data, the housekeeping gene (S18) was compared with the takeoff cycle (CT) of the LOX gene of interest (sense: 5′-CCTGGCTGTTATGATAC-3′ and antisense: 5′-GAGGCATACGCATGATG-3′), and relative gene expression was quantified using the $2^{-\Delta\Delta CT}$ method.

HPLC. HPLC samples were digested in 200 μL of 6 N of HCl at 100 °C for 18 h. Following digestion, samples were dried using a vacuum concentrator and resuspended in a solution of 10 nmol of pyridoxine per milliliter and 2.4 μmol of homoarginine per milliliter. Samples were subsequently diluted fivefold with 0.5% heptafluorobutyric acid in 10% acetonitrile and analyzed using reverse phase chromatography. From each sample, 30 μL was injected into the reverse phase column and eluted using a solvent profile described previously (64). The fluorescence intensity at 400 nm was used to quantify the amount of hydroxylysyl-PYR. PYR standards (Quidel) were also analyzed using this HPLC protocol to generate a standard curve, and subsequently determine the hydroxylysyl-PYR content of each sample.

Creep Indentation Testing. Compressive properties were evaluated using creep indentation as previously described (62). Specimens were equilibrated in PBS for 15 min, 0.2 g of tare mass was applied until equilibrium, and samples were then indented to an ∼15% strain using a flat, porous indenter tip (0.8-mm diameter). The compressive properties of the samples were obtained using a semianalytical, seminumeric, linear biphasic model (65).

Tensile Testing. Tissue tensile properties were measured via a uniaxial testing apparatus (model 5565; Instron). Samples were punched in dog-bone shapes at a 1-mm gauge length. The central region of the medial meniscus was tested in the circumferential direction. Sample thickness and width, determined using ImageJ, were as follows: neocartilage, 0.55 ± 0.14 mm and 0.73 ± 0.15 mm; native cartilage, 0.62 ± 0.33 mm and 2.02 ± 0.36 mm; meniscus, 0.76 ± 0.11 mm and 1.12 ± 0.15 mm; ligaments, 1.33 ± 0.18 mm and 1.16 ± 0.14 mm; and tendons, 1.56 ± 0.19 mm and 1.41 ± 0.20 mm, respectively. Samples were gripped on either end and loaded in tension at 0.5 mm per minute to a load of 0.02 N and then allowed to equilibrate before extension to failure at a rate of 1% per second of gauge length using a 5-kN load cell. The tensile load applied to the samples resulted in force-displacement curves, from which data were normalized to generate stress–strain curves. Young's modulus was determined from the linear region of the stress–strain curve, whereas UTS was determined at peak stress.

Quantitative Evaluation of SEM Images. Samples were prepared and evaluated as previously described (8, 66, 67). Each sample was fixed in 3% glutaraldehyde for 12 h at 4 °C. Samples were then dehydrated in ethanol, critical point-dried, sputter-coated, and imaged using a Philips XL30 TMP scanning electron microscope. Three samples were imaged for each group, with three locations of various depths imaged per sample. Images were imported into ImageJ, and a 5 × 5 grid was laid over each image. Three squares were randomly selected per image and analyzed using the threshold and measure functions of the software to quantify collagen fibril density (measured as percent area) and fibril diameter.

Statistical Analyses. Data are tabulated as mean ± SD: $n = 6$–7 for each of the biomechanical and biochemical assays, $n = 3$–4 for gene analysis, and $n = 3$ for SEM. ANOVA was used for intergroup comparisons, and Fischer's post hoc testing was applied when warranted. For each analysis, P values are indicated; for all figures, statistical significance is indicated by bars not sharing the same letters.

ACKNOWLEDGMENTS. We thank Regina F. MacBarb, PhD, and veterinary pathologists Natalia Vapniarski-Arzi, DVM, DACVP, and Denise Imai, DVM, PhD, DACVP, for their help. Funding support was received from NIH Grants R01DE019666 and R01AR053286.

1. Hu JC, Athanasiou KA (2006) A self-assembling process in articular cartilage tissue engineering. *Tissue Eng* 12(4):969–979.
2. Huey DJ, Hu JC, Athanasiou KA (2012) Unlike bone, cartilage regeneration remains elusive. *Science* 338(6109):917–921.
3. Elder BD, Athanasiou KA (2008) Synergistic and additive effects of hydrostatic pressure and growth factors on tissue formation. *PLoS ONE* 3(6):e2341.
4. Gemmiti CV, Guldberg RE (2006) Fluid flow increases type II collagen deposition and tensile mechanical properties in bioreactor-grown tissue-engineered cartilage. *Tissue Eng* 12(3):469–479.
5. Natoli RM, Revell CM, Athanasiou KA (2009) Chondroitinase ABC treatment results in greater tensile properties of self-assembled tissue-engineered articular cartilage. *Tissue Eng Part A* 15(10):3119–3128.
6. Athanasiou KA, Darling EM, Hu JC (2009) *Articular Cartilage Tissue Engineering* (Morgan & Claypool, San Rafael, CA).
7. Warnock JJ, et al. (2014) Growth factor treated tensioned synoviocyte neotissues: Towards meniscal bioscaffold tissue engineering. *Vet J* 200(1):22–30.
8. MacBarb RF, Makris EA, Hu JC, Athanasiou KA (2013) A chondroitinase-ABC and TGF-β1 treatment regimen for enhancing the mechanical properties of tissue-engineered fibrocartilage. *Acta Biomater* 9(1):4626–4634.
9. Beatty MW, Bruno MJ, Iwasaki LR, Nickel JC (2001) Strain rate dependent orthotropic properties of pristine and impulsively loaded porcine temporomandibular joint disk. *J Biomed Mater Res* 57(1):25–34.
10. Athanasiou KA, Sanchez-Adams J (2009) *Engineering the Knee Meniscus* (Morgan & Claypool, San Rafael, CA).
11. Bastiaansen-Jenniskens YM, et al. (2008) Contribution of collagen network features to functional properties of engineered cartilage. *Osteoarthritis Cartilage* 16(3): 359–366.
12. Lewis PB, McCarty LP, 3rd, Kang RW, Cole BJ (2006) Basic science and treatment options for articular cartilage injuries. *J Orthop Sports Phys Ther* 36(10):717–727.
13. Siegel RC (1976) Collagen cross-linking. Synthesis of collagen cross-links in vitro with highly purified lysyl oxidase. *J Biol Chem* 251(18):5786–5792.
14. Bailey AJ, Robins SP, Balian G (1974) Biological significance of the intermolecular crosslinks of collagen. *Nature* 251(5471):105–109.
15. Eyre DR, Weis MA, Wu JJ (2008) Advances in collagen cross-link analysis. *Methods* 45(1):65–74.
16. Ahsan T, Harwood F, McGowan KB, Amiel D, Sah RL (2005) Kinetics of collagen crosslinking in adult bovine articular cartilage. *Osteoarthritis Cartilage* 13(8):709–715.
17. Williams GM, Sah RL (2011) In vitro modulation of cartilage shape plasticity by biochemical regulation of matrix remodeling. *Tissue Eng Part A* 17(1-2):17–23.
18. Buckwalter JA, Mankin HJ (1998) Articular cartilage: Tissue design and chondrocyte-matrix interactions. *Instr Course Lect* 47:477–486.
19. Kelly DJ, et al. (2007) Biochemical markers of the mechanical quality of engineered hyaline cartilage. *J Mater Sci Mater Med* 18(2):273–281.
20. Doroski DM, Brink KS, Temenoff JS (2007) Techniques for biological characterization of tissue-engineered tendon and ligament. *Biomaterials* 28(2):187–202.
21. Hunter CJ, Mouw JK, Levenston ME (2004) Dynamic compression of chondrocyte-seeded fibrin gels: Effects on matrix accumulation and mechanical stiffness. *Osteoarthritis Cartilage* 12(2):117–130.
22. Mauck RL, Seyhan SL, Ateshian GA, Hung CT (2002) Influence of seeding density and dynamic deformational loading on the developing structure/function relationships of chondrocyte-seeded agarose hydrogels. *Ann Biomed Eng* 30(8):1046–1056.
23. Responte DJ, Arzi B, Natoli RM, Hu JC, Athanasiou KA (2012) Mechanisms underlying the synergistic enhancement of self-assembled neocartilage treated with chondroitinase-ABC and TGF-β1. *Biomaterials* 33(11):3187–3194.
24. Mow VC, Hayes WC, eds (1991) *Basic Orthopaedic Biomechanics* (Raven, New York), pp 113–178.
25. Williamson AK, Chen AC, Sah RL (2001) Compressive properties and function-composition relationships of developing bovine articular cartilage. *J Orthop Res* 19(6):1113–1121.
26. Khalsa PS, Eisenberg SR (1997) Compressive behavior of articular cartilage is not completely explained by proteoglycan osmotic pressure. *J Biomech* 30(6):589–594.
27. Chen SS, Falcovitz YH, Schneiderman R, Maroudas A, Sah RL (2001) Depth-dependent compressive properties of normal aged human femoral head articular cartilage: Relationship to fixed charge density. *Osteoarthritis Cartilage* 9(6):561–569.
28. Ficklin T, et al. (2007) Articular cartilage mechanical and biochemical property relations before and after in vitro growth. *J Biomech* 40(16):3607–3614.
29. Tran-Khanh N, Hoemann CD, McKee MD, Henderson JE, Buschmann MD (2005) Aged bovine chondrocytes display a diminished capacity to produce a collagen-rich, mechanically functional cartilage extracellular matrix. *J Orthop Res* 23(6):1354–1362.
30. Metallo CM, et al. (2012) Reductive glutamine metabolism by IDH1 mediates lipogenesis under hypoxia. *Nature* 481(7381):380–384.
31. Bozec A, et al. (2008) Osteoclast size is controlled by Fra-2 through LIF/LIF-receptor signalling and hypoxia. *Nature* 454(7201):221–225.
32. Wang GL, Jiang BH, Rue EA, Semenza GL (1995) Hypoxia-inducible factor 1 is a basic-helix-loop-helix-PAS heterodimer regulated by cellular O2 tension. *Proc Natl Acad Sci USA* 92(12):5510–5514.
33. Sarkar K, et al. (2012) Hypoxia-inducible factor 1 transcriptional activity in endothelial cells is required for acute phase cardioprotection induced by ischemic preconditioning. *Proc Natl Acad Sci USA* 109(26):10504–10509.
34. Sendoel A, Kohler I, Fellmann C, Lowe SW, Hengartner MO (2010) HIF-1 antagonizes p53-mediated apoptosis through a secreted neuronal tyrosinase. *Nature* 465(7298): 577–583.
35. LeCouter J, et al. (2001) Identification of an angiogenic mitogen selective for endocrine gland endothelium. *Nature* 412(6850):877–884.
36. Schrobback K, et al. (2012) Effects of oxygen on zonal marker expression in human articular chondrocytes. *Tissue Eng Part A* 18(9-10):920–933.
37. Provot S, Schipani E (2007) Fetal growth plate: A developmental model of cellular adaptation to hypoxia. *Ann N Y Acad Sci* 1117:26–39.
38. Domm C, Schünke M, Christesen K, Kurz B (2002) Redifferentiation of dedifferentiated bovine articular chondrocytes in alginate culture under low oxygen tension. *Osteoarthritis Cartilage* 10(1):13–22.

39. Murphy CL, Sambanis A (2001) Effect of oxygen tension and alginate encapsulation on restoration of the differentiated phenotype of passaged chondrocytes. *Tissue Eng* 7(6):791–803.
40. Murphy CL, Polak JM (2004) Control of human articular chondrocyte differentiation by reduced oxygen tension. *J Cell Physiol* 199(3):451–459.
41. Lafont JE, Talma S, Murphy CL (2007) Hypoxia-inducible factor 2alpha is essential for hypoxic induction of the human articular chondrocyte phenotype. *Arthritis Rheum* 56(10):3297–3306.
42. Robins JC, et al. (2005) Hypoxia induces chondrocyte-specific gene expression in mesenchymal cells in association with transcriptional activation of Sox9. *Bone* 37(3):313–322.
43. Schipani E, et al. (2001) Hypoxia in cartilage: HIF-1alpha is essential for chondrocyte growth arrest and survival. *Genes Dev* 15(21):2865–2876.
44. Kanichai M, Ferguson D, Prendergast PJ, Campbell VA (2008) Hypoxia promotes chondrogenesis in rat mesenchymal stem cells: A role for AKT and hypoxia-inducible factor (HIF)-1alpha. *J Cell Physiol* 216(3):708–715.
45. Lennon DP, Edmison JM, Caplan AI (2001) Cultivation of rat marrow-derived mesenchymal stem cells in reduced oxygen tension: Effects on in vitro and in vivo osteochondrogenesis. *J Cell Physiol* 187(3):345–355.
46. Koay EJ, Athanasiou KA (2008) Hypoxic chondrogenic differentiation of human embryonic stem cells enhances cartilage protein synthesis and biomechanical functionality. *Osteoarthritis Cartilage* 16(12):1450–1456.
47. Erler JT, et al. (2006) Lysyl oxidase is essential for hypoxia-induced metastasis. *Nature* 440(7088):1222–1226.
48. van Vlimmeren MA, Driessen-Mol A, van den Broek M, Bouten CV, Baaijens FP (2010) Controlling matrix formation and cross-linking by hypoxia in cardiovascular tissue engineering. *J Appl Physiol* 109(5):1483–1491.
49. Duval E, et al. (2009) Hypoxia-inducible factor 1alpha inhibits the fibroblast-like markers type I and type III collagen during hypoxia-induced chondrocyte redifferentiation: Hypoxia not only induces type II collagen and aggrecan, but it also inhibits type I and type III collagen in the hypoxia-inducible factor 1alpha-dependent redifferentiation of chondrocytes. *Arthritis Rheum* 60(10):3038–3048.
50. Schietke R, et al. (2010) The lysyl oxidases LOX and LOXL2 are necessary and sufficient to repress E-cadherin in hypoxia: Insights into cellular transformation processes mediated by HIF-1. *J Biol Chem* 285(9):6658–6669.
51. Makris EA, Hadidi P, Athanasiou KA (2011) The knee meniscus: Structure-function, pathophysiology, current repair techniques, and prospects for regeneration. *Biomaterials* 32(30):7411–7431.
52. Petersen W, Tillmann B (1999) Structure and vascularization of the cruciate ligaments of the human knee joint. *Anat Embryol (Berl)* 200(3):325–334.
53. Mauck RL, Wang CC, Oswald ES, Ateshian GA, Hung CT (2003) The role of cell seeding density and nutrient supply for articular cartilage tissue engineering with deformational loading. *Osteoarthritis Cartilage* 11(12):879–890.
54. Park S, Hung CT, Ateshian GA (2004) Mechanical response of bovine articular cartilage under dynamic unconfined compression loading at physiological stress levels. *Osteoarthritis Cartilage* 12(1):65–73.
55. Malpeli M, Randazzo N, Cancedda R, Dozin B (2004) Serum-free growth medium sustains commitment of human articular chondrocyte through maintenance of Sox9 expression. *Tissue Eng* 10(1-2):145–155.
56. Williamson AK, Masuda K, Thonar EJ, Sah RL (2003) Growth of immature articular cartilage in vitro: Correlated variation in tensile biomechanical and collagen network properties. *Tissue Eng* 9(4):625–634.
57. Waldman SD, Spiteri CG, Grynpas MD, Pilliar RM, Kandel RA (2003) Long-term intermittent shear deformation improves the quality of cartilaginous tissue formed in vitro. *J Orthop Res* 21(4):590–596.
58. van der Slot-Verhoeven AJ, et al. (2005) The type of collagen cross-link determines the reversibility of experimental skin fibrosis. *Biochim Biophys Acta* 1740(1):60–67.
59. Cole BJ, Pascual-Garrido C, Grumet RC (2009) Surgical management of articular cartilage defects in the knee. *J Bone Joint Surg Am* 91(7):1778–1790.
60. US Food and Drug Administration/Center for Biologics Evaluation and Research/Center for Devices and Radiological Health (2011) Preparation of IDEs and INDs for products intended to repair or replace knee cartilage. *FDA Guidance for Industry* (Office of Communication, Outreach and Development, Rockville, MD).
61. Rankin EB, et al. (2012) The HIF signaling pathway in osteoblasts directly modulates erythropoiesis through the production of EPO. *Cell* 149(1):63–74.
62. Makris EA, MacBarb RF, Responte DJ, Hu JC, Athanasiou KA (2013) A copper sulfate and hydroxylysine treatment regimen for enhancing collagen cross-linking and biomechanical properties in engineered neocartilage. *FASEB J* 27(6):2421–2430.
63. Natoli RM, Responte DJ, Lu BY, Athanasiou KA (2009) Effects of multiple chondroitinase ABC applications on tissue engineered articular cartilage. *J Orthop Res* 27(7):949–956.
64. Bank RA, et al. (1997) Sensitive fluorimetric quantitation of pyridinium and pentosidine crosslinks in biological samples in a single high-performance liquid chromatographic run. *J Chromatogr B Biomed Sci Appl* 703(1-2):37–44.
65. Athanasiou KA, et al. (1995) Biomechanical properties of hip cartilage in experimental animal models. *Clin Orthop Relat Res* (316):254–266.
66. Riesle J, Hollander AP, Langer R, Freed LE, Vunjak-Novakovic G (1998) Collagen in tissue-engineered cartilage: Types, structure, and crosslinks. *J Cell Biochem* 71(3):313–327.
67. Segawa K, Takiguchi R (1992) Ultrastructural alteration of cartilaginous fibril arrangement in the rat mandibular condyle as revealed by high-resolution scanning electron microscopy. *Anat Rec* 234(4):493–499.
68. Eyre D (1987) Collagen cross-linking amino acids. *Methods Enzymol* 144:115–139.
69. Eleswarapu SV, Responte DJ, Athanasiou KA (2011) Tensile properties, collagen content, and crosslinks in connective tissues of the immature knee joint. *PLoS ONE* 6(10):e26178.